Biogeosciences Discuss., 10, 9043–9068, 2013
www.biogeosciences-discuss.net/10/9043/2013/
doi:10.5194/bgd-10-9043-2013

Biogeosciences Discussions
Open Access

Water availability determines branched glycerol dialkyl glycerol tetraether distributions in soils of the Iberian Peninsula

J. Menges[1], **C. Huguet**[2], **J. M. Alcañiz**[3], **S. Fietz**[4], **D. Sachse**[1], **and A. Rosell-Melé**[2,5]

[1]University of Potsdam, Institute of Earth and Environmental Sciences, Karl-Liebknecht-Str. 24–25, 14476 Potsdam-Golm, Germany
[2]Institut de Ciència i Tecnologia Ambientals, Universitat Autònoma de Barcelona, 08193 Bellaterra, Catalonia, Spain
[3]CREAF Cerdanyola del Vallés 08193, Spain and Universitat Autònoma Barcelona, Cerdanyola del Vallès 08193, Spain
[4]Stellenbosch University, Department of Earth Sciences, 7602 Stellenbosch, Western Cape, South Africa
[5]Institució Catalana de Recerca i Estudis Avançats (ICREA), Barcelona, Catalonia, Spain

Received: 18 April 2013 – Accepted: 15 May 2013 – Published: 3 June 2013

Correspondence to: C. Huguet (carme.huguet@uab.cat)

Published by Copernicus Publications on behalf of the European Geosciences Union.

Abstract

The MBT/CBT has recently gained significant attention as a novel paleotemperature proxy. It is based on the distribution of branched glycerol dialkyl glycerol tetraethers (GDGTs) in soils. The CBT quantifies the degree of cyclisation and relates to soil pH. The MBT' quantifies the degree of methylation and relates to mean annual temperature and soil pH. Combining these two indices allows estimation of mean annual temperature (MAT). However other factors such as soil water availability or moisture conditions have been suggested to influence the MBT'. To assess the effect of moisture conditions on the MBT'/CBT a set of 23 Iberian Peninsula soil samples covering a temperature range from 10–18 °C and a wide range of soil moisture regimes (405 mm to 1455 mm mean annual precipitation per year), was analyzed. We find that CBT is significantly correlated to soil pH confirming it as a robust proxy. In contrast the MBT' index was not correlated to MAT and was weakly correlated to annual mean precipitation (MAP). Instead we found a significant correlation between MBT' and the Aridity Index (AI), a parameter related to water availability in soils. The AI can explain 70 % of the residuals of MAT estimation and 50 % of the actual variation of the MBT'. This suggests that in dry environments or under moisture shortage the degree of methylation of branched GDGTs is not controlled by temperature but rather by the degree of water available. Our results suggest that the MBT/CBT index is not applicable as a paleotemperature proxy in dry subhumid to hyperarid environments.

1 Introduction

Reconstruction of temperature beyond the instrumental record is required to understand the natural modes of climate variability. However, the reconstruction of continental temperature is particularly challenging as there are few available quantitative proxies. There are a number of studies that have used microfossil assemblages based on pollen, diatoms or chironomids preserved in lake sediments (e.g. Colinvaux et al., 1996; Kurek et al., 2009; Lotter et al., 1997). Two molecular proxies initially developed in marine environments have also been shown to be applicable in lake settings, i.e. the long chain alkenones unsaturation index (U^{K}_{37}; e.g. Marlowe et al., 1984; Toney et al., 2010; Zink et al., 2001), and the TEX_{86} index based on isoprenoidal glycerol dialkyl glycerol tetraethers (GDGTs) (e.g. Blaga et al., 2009; Powers et al., 2004; Powers et al., 2010). However, in both cases, their applicability appears limited to certain lake types.

Another molecular approach put forward more recently to estimate continental mean annual temperatures (MAT) is based on the distribution of branched GDGTs (brGDGTs) in lake sediments (Fig.1b). The brGDGTs theoretically are derived from soil organisms within the lake catchment (Weijers et al., 2007). The calculation of MAT is based on the methylation (MBT index) and cyclisation (CBT index) of the brGDGTs (Weijers et al., 2007). This approach requires disentangling the effect of air temperature and soil pH on the relative abundances of brGDGTs because the degree of methylation (MBT index) is correlated to air temperature and soil pH (Weijers et al., 2007). While originally the MBT was defined to include all brGDGTs as:

$$\mathrm{MBT} = (\mathrm{Ia} + \mathrm{Ib} + \mathrm{Ic})/(\mathrm{Ia} + \mathrm{Ib} + \mathrm{Ic} + \mathrm{IIa} + \mathrm{IIb} + \mathrm{IIc} + \mathrm{IIIa} + \mathrm{IIIb} + \mathrm{IIIc}) \quad (1)$$

a simplified index that only includes the major brGDGTs was proposed by Peterse et al. (2012):

$$\mathrm{MBT}' = (\mathrm{Ia} + \mathrm{Ib} + \mathrm{Ic})/(\mathrm{Ia} + \mathrm{Ib} + \mathrm{Ic} + \mathrm{IIa} + \mathrm{IIb} + \mathrm{IIc} + \mathrm{IIIa}) \quad (2)$$

The roman numerals correspond to the abundances of the respective brGDGTs in Fig. 1b. An estimation of soil pH can be obtained by measuring the degree of cyclisation of the brGDGTs, which was defined as the CBT index (Weijers et al., 2007):

$$\mathrm{CBT} = -\mathrm{Log}((\mathrm{Ib} + \mathrm{IIb})/(\mathrm{Ia} + \mathrm{IIa}) \quad (3)$$

$$\mathrm{CBT} = 3.33 - 0.38 \times \mathrm{pH}(n = 114; R^2 = 0.70) \quad (4)$$

BGD
10, 9043–9068, 2013

Thus by using the values of CBT and MBT' we can estimate MAT as follows (Peterse et al., 2012):

$$MAT = 0.81 - 5.67 \times CBT + 31 \times MBT' (n = 176; R^2 = 0.59) \quad (5)$$

The new calibration equation by Peterse et al. (2012) has a lower correlation coefficient than the original one by Weijers et al. (2007). While the error of the calibration is somewhat larger, with a proxy error of 5 °C, the temperatures calculated appear to be more accurate for the Peterse et al. (2012) equation.

Since the brGDGTs that are produced in soils are deposited into lake or ocean sediments, the MBT/CBT proxy has been applied in a variety of marine and freshwater sites to estimate continental temperatures (e.g. Weijers et al., 2007; Rueda et al., 2009; Peterse et al., 2012). Not surprisingly however, the brGDGTs proxy is not devoid of uncertainties. There is circumstantial evidence that brGDGTs are also biosynthesized within the lake and ocean basin, not just in the catchment soils (e.g., Sinninghe-Damsté et al., 2009; Blaga et al., 2010; Tierney et al., 2010;, Fietz et al, 2011; Sun et al., 2011; Schouten et al., 2013). Furthermore, the relatively large scatter in the original calibration datasets (Weijers et al., 2007; Peterse et al., 2012) suggests that other parameters may influence the MBT/CBT and MBT'/CBT indices besides air temperature and soil pH. Moreover, a study analyzing the brGDGT distribution in geothermally heated soils around hot springs confirmed that although the MBT index is driven by soil temperature and pH, other environmental parameters such as oxygen availability or moistness could also influence the MBT-CBT relationship (Peterse et al., 2009a). A study in a spodosol in France found a variation of 12 °C in estimated MAT within a 90 cm deep profile, which could not be explained by differences in pH and temperature alone (Huguet et al., 2010a).

In a set of 59 surface soils from North America the MBT-values did not correlate with MAT ($R^2 = 0.02$), but with mean annual precipitation (MAP) when MAP < 2000 mm ($R^2 = 0.75$). This was interpreted as evidence that in arid regions MAP rather than MAT caused the variability in the MBT index (Peterse et al., 2009b). To evaluate further the effect of moisture conditions (water availability) on the MBT/CBT proxy, we have analyzed 23 surface soil samples from locations in the Iberian Peninsula which display moderate differences in MAT (10–18 °C), but cover a wide range of soil moisture regimes (MAP of 405–1455 mm).

2 Material and methods

2.1 Samples and sites

A suite of 23 surface soil samples was collected across the Iberian Peninsula from sites with mean annual temperature (MAT) between 10° and 18 °C, and mean annual precipitation (MAP) between 405 mm and 1455 mm (Table 1; Ninyerola et al., 2005). In the Iberian Peninsula, the highest precipitation and cooler temperatures occur generally in the northwest, especially at high elevation, while the driest and warmest areas are in the southeast. A value of the aridity index (AI = MAP/Mean Annual Potential Evapotranspiration) was calculated for each site using the approach by the Consortium for Spatial Information (CGIAR-CSI) based on UNEP (1997) criteria (Tables 1 and 2; Trabucco and Zomer, 2009). For each site, soil moisture regimes were established according to Soil Survey Staff (2010). In general, the eastern Iberian Peninsula is dominated by soils developed on calcareous parent material or with a significant accumulation of calcium carbonate within the soil profile, while western soils are usually silicic, developed on magmatic or metamorphic rocks, or acidified by leaching. Soils were classified according to the Soil Taxonomy System (Soil Survey Staff, 2010) at group level, as only the surface mineral soil material was collected (Table 1). The sample set includes a wide range of soil types, belonging to 5 orders and 14 groups, covering a wide range of parent materials, and climatic and geographic conditions.

Each soil sample was obtained from the combination of three subsamples taken at least 4 m a part from each other and within a 10 m radius area. Subsamples were retrieved after removing the litter and loose gravel if present, scooping the soil from a

BGD
10, 9043–9068, 2013

depth of approximately 5 cm within a 20 × 20 cm^2 surface area, and transferring it into an aluminum tray. The soil samples were homogenized and air dried. A subsample of 500 g was then sieved (2 mm mesh size) removing vegetation remains (e.g., roots, twigs) and small stones.

2.2 Ancillary measurements

The total organic carbon (TOC) was estimated by the loss on ignition (LOI) technique in triplicate. The method was adapted from Heiri et al. (2001) heating a soil subsample at 550 °C to prevent loss of carbonates (which takes place above 700 °C). Small aluminum trays were dried for 1 h at 105 °C to eliminate hygroscopic residual water, then let to cool down for 30 min in the desiccator and weighted. One 1 g of sample was placed on the tray and dried at 105 °C for 15 h, cooled in the desiccator for 30 min and weighted to obtain dry sample weight. Finally samples were placed in the oven at 550 °C for 4 h, cooled in the desiccator and weighted. TOC was calculated from the difference between the combusted and the dry sample weight (Heiri et al., 2001) and was further corrected by a factor of 2 to account for loss of organic matter other than C. It is assumed that C represents a bit more than 50 % of soil organic matter but the correction factor is adjusted to 2 so that it compensates for the weight loss of some none-organic matter.

Soil pH was measured in 1 : 5 (soil : distilled water) suspension created after vigorous shaking of the mixture for 1 min and a settling time of 30 min (Thomas, 1996). A triplicate measurement was taken using a pH meter (GLP22, Crison Instruments) after calibration of the electrode with standard solutions at pH 4 and 7.

2.3 GDGTs analysis

Samples of approximately 1 g of dry soil were spiked with an internal standard (GR) after weighing them. The total extractable lipid content was obtained using a microwave with a solvent mixture of dichloromethane (DCM): methanol (MeOH) (3 : 1,

BGD
10, 9043–9068, 2013

$v:v$). The temperature of the vessel containing the soil aliquot was increased to 70 °C over 5 min, held at 70 °C for 5 min and then decreased to 30 °C. The supernatant of the obtained solution was collected and dried under a stream of nitrogen. The total extracts were then separated into three fractions of different polarity according to the method in Huguet et al. (2010b). In short, a column filled with activated silica containing the lipid extract was eluted with the following solvents: n-hexane, dichloromethane and methanol. The methanol fraction contained the GDGTs, was then evaporated under N_2, redissolved in hexane:n-propanol (99 : 1, v/v) and filtered through 0.45 µm polyvinylidene difluouride (PTFE) filters previous to analysis by high performance liquid chromatography-mass spectrometry (HPLC-MS). The analysis was performed using a Dionex P680 HPLC system coupled to a Thermo Finnigan Quantum Discovery Max triple sector quadrupole mass spectrometer with an atmospheric pressure chemical ionization (APCI) interface set in positive mode. Instrumental and chromatographic conditions were adopted from Schouten et al. (2007), Escala et al. (2009) and Fietz et al. (2011). Extracts were eluted using a Prevail Cyano column (2.1 × 150 mm, 3 mm; Alltech) fitted with a guard column. The flow rate was set at 0.6 mL min^{-1} and the HPLC program was as follows: 98.5 % hexane and 1.5 % *n*-propanol for 4 min, increasing the proportion of *n*-propanol to 5 % in 11 min, then to 10 % over a minute and held constant for 4 min, and finally lowered to 1.5 % in 1 min and held constant for a further 9 min prior to injecting the next sample. The parameters of the APCI were set as follows to generate positive ion spectra: corona discharge 3 mA, vaporizer temperature 400 °C, sheath gas pressure 49 mTorr, auxiliary gas (N_2) pressure 5 mTorr and capillary temperature 200 °C. GDGTs were detected in selected ion monitoring (SIM) mode of $[M+H]^+ \pm 0.5\ m/z$ units. Absolute abundances of the brGDGTs were quantified by comparison of the corresponding peak areas with those of the internal standard GR and correcting for the response factor (cf. Huguet et al., 2006).

The reproducibility of the measurement of MBT' and CBT was 0.0063 and 0.0217 respectively, and obtained by repeated analysis (6 times) of soil sample X-Ref (Fig. 1a). The confidence interval for the MBT' and CBT was set at 99 %. The possibility of an apparent correlation between abundance and MBT' and CBT due to an increased analytical error at low abundances was excluded by establishing an imaginary threshold setting all peaks with an area below 5×10^4 to zero and recalculating the MBT' and CBT. Comparison of the recalculated MBT' and CBT with the former ones did not reveal substantial deviations. ($R^2 = 0.96$, $R^2 = 0.99$ respectively). Moreover we used the simplified MBT' index (Peterse et al., 2012) to avoid bias due to lack of the less abundant brGDGTs (IIIb and IIIc, Fig. 1).

All estimated values based on the GDGT are indicated by subscript "est" all instrumentally measured values are indicated by subscript "im". The residuals where calculated by subtracting the estimated MAT (MAT_{est}, using the MBT') and pH (pH_{est}, using CBT) from the instrumentally measured MAT (MAT_{im}) and soil pH (pH_{im}).

3 Results and discussion

3.1 BrGDGT abundances and distribution

The concentrations of brGDGTs ranged between 1.2 ng g^{-1}_{TOC} and 43.3 ng g^{-1}_{TOC} (Table 2). Soils with the highest absolute brGDGT abundances were located in the northern Iberian Peninsula, the area with the highest rainfall and cooler temperatures. Towards the drier and warmer south the brGDGT abundances gradually decreased (Table 2). The highest brGDGT abundance was found in an Endoaquoll (sample code CAR, Tables 1 and 2), a relative singular soil with aquic moisture regime, formed on an alluvial delta with a high LOI value (9 %), and with relatively high mean annual precipitation (MAP_{im}) in our data set (886 mm) (Tables 1 and 2). In fact this sample is unusual in our data set as its abundance in brGDGT is one order of magnitude higher than in most of the others (Table 2). We have considered it an outlier and excluded it from subsequent statistical analysis.

High brGDGT abundances were also found in soil types Hapludoll (1 sample) and Dystrudept (4 samples). These soils are associated with high MAP_{im} values and LOI %

Discussion Paper | Discussion Paper | Discussion Paper | Discussion Paper |

BGD
10, 9043–9068, 2013

Title Page
Abstract | Introduction
Conclusions | References
Tables | Figures
◀| |▶
◀ ▶
Back | Close
Full Screen / Esc
Printer-friendly Version
Interactive Discussion

values above average. In fact the CER soil has the highest LOI (18.3 %) in the study area (Tables 1 and 2). Thus our data suggest that brGDGT abundance is controlled by both precipitation and to a lesser extent by TOC abundance. Soils with high water content may easily become anoxic, thus potentially providing an ideal environment for brGDGT source organisms. The organisms that synthesize brGDGTs are still not known, but based on brGDGT structure and distributions they are hypothesised to be anoxic acidophile bacteria (Weijers et al., 2006). Earlier studies showed that brGDGT abundances are usually high in water saturated soils and peat bogs, most likely because the source organisms are anaerobic (Weijers et al., 2006). So far brGDGT were identified in only two aerobic *Acidobacteria* species suggesting that the brGDGT are likely synthesized by different bacterial communities (e.g. anaerobic and aerobic; Sinninghe-Damsté et al., 2011). However, despite covering a pH range from 4.8 to 8.7, we do not see an increase in brGDGTs with lower pH contradicting earlier findings (e.g. Peterse et al., 2010; Sinnghe-Damsté et al., 2011; Yang et al., 2011). This may indicate that *Acidobacteria* are not necessarily the main source of brGDGTs in Iberian soils.

BrGDGTs source organisms were also suggested to be heterotrophic (Weijers et al., 2010), which could explain the higher brGDGTs abundance with high organic carbon content in our dataset. In fact, high brGDGTs abundances have been previously found in peat bogs, which apart from being water logged (anoxic conditions), have high organic carbon contents (Weijers et al., 2006). In addition soil organic matter increases the capacity of soil to hold plant available water (Brady and Weil, 2002), thus providing additional moisture and possibly enhancing brGDGT production.

The predominant brGDGT is GDGT IIa, followed by IIIa and Ia (Table 2). The brGDGT's IIIb and c as well as brGDGT IIc are only present in minor amounts. In eight of the samples (35 % of the total) none of these brGDGTs are present, or their concentration is below the detection limit (Table 2) agreeing with previous results for 278 globally distributed soils (Peterse et al., 2012).

3.2 pH estimations using CBT index

In the soils studied, the CBT values range from 0.23 to 1.71 with an average of 0.81 (Table 1). Even though this is a regional study, our CBT values span almost 70 % of those published previously in Weijers et al. (2007) global calibration set. CBT values and pH_{im} of the Iberian soils are linearly correlated showing a similar slope (−0.33) to the one determined in the global calibration set (−0.35, Peterse, 2012; Weijers, 2007; Fig. 2a). Many CBT values in the Spanish data set underestimate the pH_{im} (Fig. 3a), and we therefore assume that either additional environmental parameters are influencing the degree of cyclisation or a different brGDGT producing community is dominant in the Iberian Peninsula compared to the global data set. However, when other parameters were tested, no correlation was observed between CBT and MAP_{im}, MAT_{im} (Fig. 2b and c) or LOI %, thus suggesting that they do not control brGDGT cyclisation. It is possible that additional soil parameters not taken into account in this study may affect the CBT estimate. However, the pH_{est} residuals are still randomly distributed (Fig. 3b), indicating no one single factor causing the CBT bias.

3.3 Temperature estimates using MBT' index

Instrumentally measured air temperatures in the areas considered in this study range from 3–23 °C. When annual mean values (MAT_{im}) are calculated the range is reduced to 10–18 °C. The MBT' values in the Iberian soils vary from 0.09 (relating to a MAT_{est} of −0.9 °C) to 0.59 (relating to a MAT_{est} of 9.4 °C) and have an average of 0.28 (relating to a MAT_{est} of 4.95 °C) (Table 1) thus well below instrumentally measured temperatures. As previous studies indicated that the variation in the MBT index is mostly explained by differences in soil pH and temperature (Weijers et al., 2007), we compared the MBT' values of our samples to measured pH (pH_{im}) and temperature (MAT_{im}) (Fig. 2d and e). We observe a significant correlation between measured pH and MBT' values which is higher than the one observed in the global data set (Fig. 2d). Thus, pH clearly influences the MBT' in the study area. Regarding temperatures, while the MBT' values of

BGD
10, 9043–9068, 2013

the Iberian soils fall within published values for global data (Peterse et al., 2012), we observe a similarly large range in MBT' values (from 0.09 to 0.6) for a much narrower range of temperatures (10–18 °C; Fig. 2e). Interestingly, MBT' and MAT_{est} show a weak but significant inverse correlation within the Spanish sample set (R^2 = 0.21; P = 0.02) in contrast to the normal correlation between MBT and MAT observed by Weijers et al. (2007) and Peterse et al. (2012) (Fig. 2e). Therefore, contrary to the global data set, the relative abundance of methyl brGDGTs increases at higher temperatures. However, since the temperature range over our dataset with 8 °C is just above the proxy uncertainty of 5 °C, we do not regard this inverse correlation as evidence for a causal relationship. Instead, our observations provide strong evidence that temperature is not the dominant control on the MBT' index in Spanish soils.

MAT_{est} values in 17 out of the 23 soil samples underestimate the MAT_{im} by more than the 5 °C proxy error (Fig. 3c, Table 1). For example, a soil sample close to the Zarracatín lagoon in the south of Spain (sample code ZA, Table 2), where monthly mean temperatures never fall below 11 °C and MAT_{im} is 18 °C, has a MAT_{est} value of 1.9 °C (Table 1). Even if we were to attempt a regional calibration of the MBT', the weak correlation between MBT' and MAT_{im} observed would result in an error much higher than the 5 °C reported for the global data set (Peterse et al., 2012). Moreover, local calibrations have already been proven not to improve MBT'/CBT accuracy (Peterse et al., 2012). These findings constrain the use of the MBT'/CBT for paleotemperature reconstructions in the Iberian Peninsula and indicate that care should be taken in other regions.

Furthermore, our results clearly indicate that MAT_{est} residuals are not randomly distributed but rather the obtained MAT_{est} values from MBT' are overestimated below 10 °C and overestimated for those temperatures above (Fig. 3d). This bi-directional deviation has been observed previously in the global data set (Peterse et al., 2012) but it is more extreme in the Iberian soils (Fig. 3d). We interpret this result to mean there is an additional factor influencing the MBT' index. A recent study attributed the lack of correlation between MAT_{im} and MBT/CBT to factors such as vegetation change and changes in

BGD
10, 9043–9068, 2013

hydrologic moisture regime (Weijers et al., 2011), therefore we investigated the effect of MAP on the MBT' in our samples.

3.4 Potential control of MAP on the MBT' in Spanish soils

The samples where the MBT' derived temperature is over or underestimated by more than 5 °C, originate from dry environments and we observe a statistically significant correlation between the MBT' and MAP_{im} ($R^2 = 0.52$, $P < 0.0001$; Fig. 2f). Previously the MBT vs. MAP_{im} correlation was interpreted as the result of covariation between temperature and precipitation and it was argued against causality between MBT and MAP_{im} (Weijers et al., 2007). This effect may be true for tropical sites in the global dataset, where more precipitation is often associated with higher temperatures. Arid regions, such as the southern Iberian Peninsula, do not correspond to such a pattern, as the highest temperatures are found in the driest areas. Instead, for the Iberian soil dataset we find a weak inverse correlation between MAP_{im} and MAT_{im} ($MAT_{im} = -0.0004\,MAP_{im} + 16$, $R^2 = 0.32$) like is the case for the MBT' and MAT_{im} (Fig. 2e). Consequently, within the Iberian soils, the correlation of the MBT' and MAP_{im} cannot be caused by a covariation of temperature and precipitation. Instead our results suggest that site-specific water availability possibly influenced the MBT' in the Iberian soils. Peterse et al. (2012) already suggested an effect of precipitation on the MBT' index because the addition of temperate soil data to the global data set increased the scatter of the original MBT calibration (Weijers et al., 2007). This can be better visualized by plotting only data in the 8–20 °C range (Fig. 3c insert). It becomes evident that even though the positive slope of the Peterse et al. (2012) data plot remains, the data show a large scatter, with an R^2 of 0.09, much lower than the R^2 of 0.58 of the global data set. Therefore the MBT' performs poorly in this temperate soil range regardless of the study area and this should be taken into account in future regional studies.

Interestingly both the brGDGTs abundance normalized to TOC and the MAT_{est} residuals are significantly correlated with MAP_{im} (Fig. 4a and c). This may indicate that under water stress the brGDGT-producing organisms are less productive and may have

BGD
10, 9043–9068, 2013
Water availability determines brGDGTs distribution
J. Menges et al.

to adapt their membranes to water availability rather than temperature resulting in the observed underestimation of MAT_{est}. Our data show that brGDGT abundance is significantly lower under dryer (Table 2) and potentially oxic conditions.

The physiological influence of changes in hydrological conditions on the degree of methylation of the brGDGTs is not yet known. We present two hypotheses, (I) indirectly through altering soil pH and (II) directly by constraining water availability and defining redox conditions.

(I) It is possible that precipitation has an indirect influence on the MBT' as the amount of precipitation can affect soil pH due to increased leaching of calcium and magnesium (Brady and Weil, 2002). Additionally, rainwater has a slightly acidic pH of 5.7 due to the dissolution of atmospheric CO_2 (Brady and Weil, 2002). But no correlation was observed between CBT (or pH_{im}) and MAP_{im} at the investigated sites (Fig. 2c). Hence, a possible effect of precipitation on soil pH cannot explain the correlation between MAT_{est} residuals and precipitation.

(II) Precipitation is only one expression of hydrological conditions at a site, as the water available for organisms is also influenced by soil type, vegetation and water circulation through percolation and evaporation. We tested for a possible effect of soil type, but could not find a significant correlation with MBT'. Nonetheless, Dystrudept and Hapludoll were found to have some of the highest brGDGT abundances and a good agreement between MAT_{est} and MAT_{im}.

As the correlation with MAP_{im} is stronger for brGDGT abundances (R^2 =0.68) than for the MAT_{est} residuals (R^2 = 0.59) (Fig. 4a and b), we suggest that brGDGT abundance is not the key factor to explain the MBT'-MAT_{est} scatter in our dataset. Water availability is critical in semiarid soils affecting osmotic status, abundance of microbial cells as well as nutrient cycling (Bustamante et al., 2012 and references therein). In order to better estimate water availability we used the aridity index (AI), a measure for moisture availability in soils excluding the specific impact of soil condition to adsorb and hold water (Trabucco and Zomer, 2009). The AI is a ratio of MAP and mean annual potential evaporation and increases for more humid conditions (see Trabucco and Zomer, 2009 for details).

In the Iberian soils the brGDGTs abundance shows a significant correlation with the AI (Fig. 4b), but the AI is stronger correlated with the MAT_{est} residuals (Fig. 4d). In fact, the AI can explain 70 % of the variance in the residuals (Fig. 4d), and 50 % of the variance in the MBT' index. This suggests soil moisture availability, rather than precipitation, as the main factor influencing the MBT' index besides temperature and pH. However the AI cannot explain all the variation observed in the MBT' and other factors such as vegetation type or soil water retention capacity that also affect water availability most probably play a role. In fact vegetation type has already been shown to affect the MAT_{est} values in USA soils (Weijers et al., 2011).

Our results have significant implications for the interpretation of paleotemperature records derived from the MBT/CBT index. Based on our analysis, we urge caution that below an aridity index of ca. 0.8, which includes all dry-subhumid to hyperarid environments, the deviation of MAT_{est} becomes larger than the average 5 °C proxy uncertainty. While the exact hydrological threshold below which water availability exerts a stronger control on the MBT/CBT index than temperature will have to be determined in future studies, we recommend that hydrological conditions should be evaluated in conjunction with MBT/CBT paleotemperatures, for example through paleohydrological proxies (see Sachse et al., 2012 for proxy details).

4 Conclusions

When the distribution of brGDGTs was analyzed in soils from the Iberian Peninsula, the CBT index was shown to covary with soil pH with sufficient accuracy to confirm its use as proxy for estimating paleo-soil pH. The MBT' index was also shown to relate to soil pH, but the expected relation between MBT' and MAT_{im} was not apparent. Due to these results the application of MBT'/CBT proxy to estimate air temperatures does not seem appropriate in the Iberian Peninsula. Instead of being correlated to temperature

BGD
10, 9043–9068, 2013

the MBT' index was shown to be coupled with precipitation and the aridity index (AI). This suggests that under moisture shortage the degree of methylation of brGDGTs is not coupled to temperature and is instead controlled by soil water availability. These findings should be taken into account when interpreting MBT/CBT climatic records from dry-subhumid, semi-arid and arid areas.

Acknowledgements. We want to thank Ferran Colomer Ventura for LOI % measurements and sampling map. Núria Moraleda and Gemma Rueda are thanked for technical assistance. This work was financed through the Juan de la Cierva grants from the Spanish government to C. H and S. F. The work leading to these results has received funding from the European Union Seventh Framework Programme (FP7/2007-2013) under grant agreement no. [252659].

References

Bendle, J. A., Weijers, J. W. H., Maslin, M. A., Sinninghe Damsté, J. S., Schouten, S., Hopmans, E. C., Boot, C. S., and Pancost, R. D.: Major changes in glacial and Holocene terrestrial temperatures and sources of organic carbon recorded in the Amazon fan by tetraether lipids, Geochem. Geophys. Geosyst., 11, Q12007, doi:10.1029/2010GC003308, 2010.

Blaga, C. I., Reichart, G. J., Heiri, O., and Sinninghe Damsté, J. S.: Tetraether membrane lipid distributions in water-column particulate matter and sediments: a study of 47 European lakes along a north-south transect, J. Paleolimnol., 41, 523–540, 2009.

Blaga, C. I., Reichart, G. J., Schouten, S., Lotter, A. F., Werne, J. P., Kosten, S., Mazzeo, N., Lacerot G., and Sinninghe Damsté, J. S.: Branched glycerol dialkyl glycerol tetraethers in lake sediments: Can they be used as temperature and pH proxies?, Org. Geochem., 41, 1225–1234, 2010.

Brady, N. C. and Weil, R. R.: The Nature and Properties of Soils, 13th edition. Prentice Hall. Upper Saddle River, New Jersey, 960 pp., 2002.

Bustamante, M. M. C. Nardoto, G. B., Pinto, A. S., Resende, J. C. F., Takahashi, F. S. C., and Vieira, L. C. G.: Potential impacts of climate change on biogeochemical functioning of Cerrado ecosystems, Brazil. J. Biol., 72, 655–671, 2012.

Colinvaux, P. A., DeOliveira, P. E., Moreno, J. E., Miller, M. C., and Bush, M. B.: A long pollen record from lowland Amazonia: Forest and cooling in glacial times, Science, 274, 85–88, 1996.

Escala, M., Fietz, S., Rueda, G., and Rosell-Melé, A.: Analytical Considerations for the Use of the Paleothermometer Tetraether Index(86) and the Branched vs Isoprenoid Tetraether Index Regarding the Choice of Cleanup and Instrumental Conditions, Anal. Chem., 81, 2701–2707, 2009.

Fietz, S., Martinez-Garcia, A., Huguet, C., Rueda, G., and Rosell-Mele, A.: Constraints in the application of the Branched and Isoprenoid Tetraether index as a terrestrial input proxy, J. Geophys. Res.-Oceans, 116, C10032, doi:10.1029/2011JC007062, 2011.

Heiri, O., Lotter, A. F., and Lemcke, G.: Loss on ignition as a method for estimating organic and carbonate content in sediments: reproducibility and comparability of results, J. Paleolimnol., 25, 101–110, 2001.

Huguet, C., Hopmans, E. C., Febo-Ayala, W., Thompson, D. H., Sinninghe Damsté, J. S., and Schouten, S.: An improved method to determine the absolute abundance of glycerol dibiphytanyl glycerol tetraether lipids, Org. Geochem. 37, 1036–1041, 2006.

Huguet, A., Fosse, C., Laggoun-Defarge, F., Toussaint, M.-L., and Derenne, S.: Occurrence and distribution of glycerol dialkyl glycerol tetraethers in a French peat bog, Org. Geochem., 41, 559–572, 2010a.

Huguet, C., Martens-Habbena, W., Urakawa, H., Stahl D. A., and Ingalls, A. E.: Optimization of extraction methods for intact and core glycerol dialkyl glycerol tetraethers (GDGTs), Limnol. Oceanogr.-Methods, 8, 127–145, doi:10.4319/lom.2010.8.127, 2010b.

Kurek, J., Cwynar, L. C., Ager, T. A., Abbott, M. B., and Edwards, M. E.: Late Quaternary paleoclimate of western Alaska inferred from fossil chironomids and its relation to vegetation histories, Quat. Sci. Rev., 28, 799–811, 2009.

Lotter, A. F., Birks, H. J. B., Hofmann, W., and Marchetto, A.: Modern diatom, cladocera, chironomid, and chrysophyte cyst assemblages as quantitative indicators for the reconstruction of past environmental conditions in the Alps .1. Climate, J. Paleolimnol., 18, 395–420, 1997.

Marlowe, I. T., Green, J. C., Neal, A. C., Brassell, S. C., Eglinton, G., and Course, P. A.: Long-chain (N-C37-C39) alkenones in the Prymnesiophyceae – distribution of alkenones and other lipids and their taxonimic significance, Brit. Phycol. J., 19, 203–216, 1984.

BGD
10, 9043–9068, 2013

Ninyerola, M., Pons, X., and Roure, J. M.: Atlas climático digital de la Península Ibérica, Metodología y aplicaciones en bioclimatología y geobotánica, Universitat Autònoma de Barcelona, Bellaterra, 2005.

Peterse, F., Schouten, S., van der Meer, J., van deer Meer, M. T. J., and Sinninghe Damsté, J. S.: Distribution of branched tetraether lipids in geothermally heated soils: implications for the MBT/CBT temperature proxy, Org. Geochem., 40, 201–205, 2009a.

Peterse, F., Schouten, F., Fierer, N., Jackson, R. B., Nicol, G. W., Weijers, J. W. H., van Groeningen, K. J., Wiesenberg, G. L. B., Jia, G., and Sinninghe Damsté, J. S.: Environmental controls on the bacterial tetraether membrane lipid distribution in soils: implications for the MBT/CBT temperature proxy, in: 24th Internationa Meeting on Org. Geochem., Bremen, Germany, p. 72 (abstract), 2009b.

Peterse, F., Nicol, G. W., Schouten, S., and Sinninghe Damsté, J. S.: Influence of soil pH on the abundance and distribution of core and intact polar lipid-derived branched GDGTs in soil, Org. Geochem., 41, 1171–1175, 2010.

Peterse, F. Meer, J. van der, Schouten, S., Weijers, J. W. H., Fierer, N., Jackson, R. B., Kim, J.-H., Sinninghe Damsté, J. S.: Revised calibration of the MBT-CBT paleotemperature proxy based on branched tetraether membrane lipids in surface soils, Geochim. Cosmochim. Ac., 96, 215–229, 2012.

Powers, L. A., Werne, J. P., Johnson, T. C., Hopmans, E. C., Sinninghe Damsté, J. S., and Schouten, S.: Crenarchaeotal membrane lipids in lake sediments: A new paleotemperature proxy for continental paleoclimate reconstruction?, Geology, 32, 613–616, 2004.

Powers, L., Werne, J. P., Vanderwoude, A. J., Sinninghe Damsté, J. S., Hopmans, E. C., and Schouten, S.: Applicability and calibration of the TEX_{86} paleothermometer in lakes, Org. Geochem., 41, 404–413, 2010.

Rueda, G., Rosell-Mele, A., Escala, M., Gyllencreutz, R., and Backman, J.: Comparison of instrumental and GDGT-based estimates of sea surface and air temperatures from the Skagerrak. Org. Geochem., 40, 287–291, 2009.

Sachse, D., Billault, I., Bowen, G. J., Chikaraishi, Y., Dawson, T. E., Feakins, S. J, Freeman, K. H., Magill, C. R., McInerney, F. A., van der Meer, M. T. J., Polissar, P., Robins, R. J., Sachs, J. P., Schmidt, H.-L., Sessions, A. L., White, J. W. C., West, J. B., and Kahmen, A.: Molecular Paleohydrology: Interpreting the Hydrogen- Isotopic Composition of Lipid Biomarkers from Photosynthesizing Organisms, Annu. Rev. Earth Planet. Sci., 40, 221–249, 2012.

Schouten, S., Huguet, C., Hopmans, E. C., Kienhuis, M. V. M., and Sinninghe Damsté, J. S.: Analytical methodology for TEX_{86} paleothermometry by highperformance liquid chromatography/atmospheric pressure chemical ionization-mass spectrometry, Anal. Chem., 79, 2940–2944, 2007.
Schouten, S., Hopmans, E. C., and Sinninghe Damsté, J. S.: The organic geochemistry of glycerol dialkyl glycerol tetraether lipids: A review, Org. Geochem., 54, 19–61, 2013.
Sinninghe-Damsté, J. S., Ossebaar, J., Abbas, B., Schouten, S., and Verschuren, D.: Fluxes and distribution of tetraether lipids in an equatorial African lake: Constraints on the application of the TEX_{86} palaeothermometer and BIT index in lacustrine settings, Geochim. Cosmochim. Ac., 73, 4232–4249, 2009.
Sinninghe-Damsté, J. S., Rijpstra, W. I. C., Hopmans, E. C., Weijers, J. W. H., Foesel, B. U., Overmann, J., and Dedysh, S. N.: 13,16-Dimethyl Octacosanedioic Acid (iso-Diabolic Acid), a Common Membrane-Spanning Lipid of Acidobacteria Subdivisions 1 and 3, Appl. Environ. Microbiol., 77, 4147–4154, 2011.
Soil Atlas of Europe: European Soil Bureau Network European Commission, Office for Official Publications of the European Communities, L-2995 Luxembourg, 128 pp., 2005.
Soil Survey Staff: Keys to Soil Taxonomy (Eleventh Edn.), United States Department of Agriculture, Natural Resources Conservation Service, 338 pp., 2010.
Sun, Q., Chu, G., Liu, M., Xie, M., Li, S., Ling, Y., Wang, X., Shi, L., Jia, G., and Lü, H.: Distributions and temperature dependence of branched glycerol dialkyl glycerol tetraethers in recent lacustrine sediments from China and Nepal, J. Geophys. Res. 116, G01008, doi:10.1029/2010JG001365, 2011.
Thomas, G. W.: Soil pH and soil acidity, in: Methods of soil analysis. Part 3 Chemical methods, SSSA Books series: 5 SSSA, edited by: Bartels, J. M., Madison, WI, 1996.
Tierney, J. E., Russell, J. M., Eggermont, H., Hopmans, E. C., Verschuren, D., and Sinninghe Damsté, J. S.: Environmental controls on branched tetraether lipid distributions in tropical East African lake sediments, Geochim. Cosmochim. Ac., 74, 4902–4918, 2010.
Toney, J. L. Huang, Y. S., Fritz, S. C., Baker, P. A., Grimm, E., and Nyren, P.: Climatic and environmental controls on the occurrence and distributions of long chain alkenones in lakes of the interior United States, Geochim. Cosmochim. Ac., 74, 1563–1578, 2010.
Trabucco, A. and Zomer, R. J.: Global Aridity Index (Global-Aridity) and Global Potential Evapo-Transpiration (Global-PET) Geospatial Database. CGIAR Consortium for Spatial Informa-

tion, Published online, available from the CGIAR-CSI GeoPortal at: http://www.csi.cgiar.org, 2009.

UNEP: United Nations Environment Program, World Atlas of Desertification, 2nd Edn., UNEP, London, 1997.

Weijers, J. W. H., Schouten, S., Hopmans E. C., Geenevasen, J. A. J., David, O. R. P., Coleman, J. M., Pancost, R. D., and Sinninghe Damsté, J. S.: Membrane lipids of mesophilic anaerobic bacteria thriving in peats have typical archaeal traits, Environ. Microbiol., 8, 648–657, 2006.

Weijers, J. W. H., Schouten, S., van den Donker, J. C., Hopmans, E. C., and Sinninghe Damsté, J. S.: Environmental controls on bacterial tetraether membrane lipid distribution in soils, Geochim. Cosmochim. Ac., 71, 703–713, 2007.

Weijers, J. W. H., Wiesenberg, G. L. B., Bol, R., Hopmans, E. C., and Pancost, R. D.: Carbon isotopic composition of branched tetraether membrane lipids in soils suggest a rapid turnover and a heterotrophic life style of their source organism(s), Biogeosciences, 7, 2959–2973, doi:10.5194/bg-7-2959-2010, 2010.

Weijers, J. W. H., Bernhardt, B., Peterse, F., Werne, J. P., Dungait, J. A. J., Schouten S., and Sinninghe Damsté, J. S.: Absence of seasonal patterns in MBT-CBT indices in mid-latitude soils, Geochim. Cosmochim. Ac., 75, 3179–3190, 2011.

Yang, H., Ding, W. H., Wang, J.-X., Jin, C.-S., He, G.-Q., Qin, Y.-M., and Xie, S.-C.: Soil pH impact on microbial tetraether lipids and terrestrial input index (BIT) in China, Sci. China Earth Sci., 54, 1–10, 2011.

Zink, K. G., Leythaeuser, D., Melkonian, M., and Schwark, L.: Temperature dependency of long-chain alkenone distributions in Recent to fossil limnic sediments and in lake waters, Geochim. Cosmochim. Ac., 65, 253–265, 2001.

BGD

10, 9043–9068, 2013

Table 1. Sample code and coordinates, mean annual temperature (MAT_{im}), mean annual precipitation (MAP_{im}), aridity index (AI), pH (pH_{im}) and loss on ignition (LOI (%)). Soils were classified according to Soil Taxonomy (Soil Survey Staff, 2010) at Group level. The calculated CBT, MBT ratios as well as derived pH (pH_{est}) and MAT estimated (MAT_{est}) are also included.

Sample	Latitude	Longitude	MAT_{im} (°C)	MAP_{im} (mm)	AI	pH_{im}	LOI (%)	Soil Group	CBT	MBT'	pH_{est}	MAT_{est} (°C)
AM	37.32	−4.62	16	509	0.50	8.7	3.7	Calcixerept	0.53	0.21	7.3	4.3
CA	42.26	−2.09	13	450	0.51	7.8	2.5	Torriorthent	0.29	0.08	7.9	1.6
CAR	42.49	−6.78	12	886	0.71	7.4	9.0	Endoaquoll	0.35	0.24	7.7	6.4
CAR-M	42.49	−6.79	12	948	0.73	6.8	3.6	Eutrudept	0.79	0.38	6.6	8.1
CAY	42.78	−2.99	11	471	0.94	6.4	10.3	Calcixeroll	1.08	0.36	5.8	5.8
CER	40.32	−5.93	12	866	0.64	4.8	18.3	Dystrudept	n.d.	0.49	n.d.	n.d.
CER-B	38.25	−4.25	15	771	0.45	6.4	2.3	Xerorthent	1.34	0.32	5.2	3.2
COV	43.30	−5.04	12	1455	0.97	6.7	6.3	Hapludoll	0.29	0.42	7.9	12.0
E	42.03	−0.53	14	494	0.45	8.4	5.8	Calcixerept	0.33	0.21	7.8	5.5
ER	43.27	−4.98	10	1443	1.13	5.1	6.1	Dystrudept	1.71	0.59	4.2	9.4
EST	41.07	−0.20	14	415	0.40	7.5	1.5	Torriorthent	0.85	0.09	6.4	−1.3
MA	39.41	−2.88	14	416	0.35	8.1	1.3	Calcixerept	0.64	0.16	7.0	2.2
MI	38.94	−4.34	14	532	0.38	6.2	2.7	Haploxeralf	1.31	0.35	5.2	4.2
MO	42.33	1.00	10	770	1.11	6.6	7.6	Haplustoll	0.63	0.34	7.0	7.8
OL	37.96	−6.28	16	776	0.51	6.2	2.6	Haplorexept	1.04	0.38	5.9	6.6
RE	41.85	−1.14	15	405	0.42	7.8	2.2	Haplogypsid	0.78	0.09	6.6	−0.9
SAL	40.62	−5.63	11	593	0.44	6.0	3.1	Haploxeralf	1.44	0.26	4.9	0.8
SAN	42.13	−6.71	10	1335	1.03	6.3	6.0	Dystrudept	1.10	0.38	5.8	6.4
SAN-C	42.13	−6.70	10	1335	0.89	5.7	4.6	Dystrudept	1.25	0.44	5.4	7.4
TA	40.65	−1.97	10	716	0.53	8.3	5.8	Calcixeroll	0.35	0.15	7.7	3.3
TO	40.55	−2.05	11	1002	0.53	8.3	7.8	Haploxeroll	0.23	0.18	8.1	4.9
ZA	37.04	−5.79	18	611	0.50	8.4	2.6	Haploxerept	0.59	0.14	7.1	1.9
ZO	37.49	−4.68	17	520	0.49	8.5	1.8	Xerarent	0.64	0.17	7.0	2.4

Table 2. Sample code and coordinates, Aridity Index (AI), individual branched GDGTs relative abundances (%) and total brGDGTs abundance related to TOC ($ng\,g_{TOC}^{-1}$), n.d. denotes not detected.

Sample	Latitude	Longitude	AI	Branched GDGTs (%)									BrGDGTs
				Ia	Ib	Ic	IIa	IIb	IIc	IIIa	IIIb	IIIc	($ng\,g_{TOC}^{-1}$)
MA	39.41	−2.88	0.35	11.9	4.4	n.d.	35.4	6.4	n.d.	41.9	n.d.	n.d.	2.1
MI	38.94	−4.34	0.38	32.6	2.4	n.d.	47.0	1.4	n.d.	16.6	n.d.	n.d.	2.4
EST	41.07	−0.20	0.40	8.7	n.d.	n.d.	42.7	7.3	n.d.	41.4	n.d.	n.d.	1.6
RE	41.85	−1.14	0.42	8.6	n.d.	n.d.	42.9	8.5	n.d.	36.6	3.5	n.d.	2.6
SAL	40.62	−5.63	0.44	25.2	1.2	n.d.	51.5	1.6	n.d.	20.5	n.d.	n.d.	2.7
CER−B	38.25	−4.25	0.45	30.4	1.7	n.d.	47.7	1.8	n.d.	18.4	n.d.	n.d.	6.2
E	42.03	−0.53	0.45	13.2	7.0	0.8	36.3	16.4	n.d.	26.3	n.d.	n.d.	2.8
ZO	37.49	−4.68	0.49	11.33	5.2	n.d.	39.5	6.5	n.d.	36.0	1.4	n.d.	2.2
AM	37.32	−4.62	0.50	10.1	6.3	3.4	31.9	6.1	n.d.	36.6	3.9	1.8	2.5
ZA	37.04	−5.79	0.50	10.4	3.4	n.d.	39.6	9.5	n.d.	34.5	2.6	n.d.	2.0
CA	42.26	−2.09	0.51	6.7	n.d.	n.d.	27.0	17.5	n.d.	36.3	12.4	n.d.	1.2
OL	37.96	−6.28	0.51	33.7	4.0	n.d.	48.1	3.4	n.d.	10.7	n.d.	n.d.	6.7
TA	40.65	−1.97	0.53	8.7	4.8	0.7	35.5	14.7	n.d.	33.0	2.2	0.2	3.6
TO	40.55	−2.05	0.53	10.0	6.5	0.4	32.1	18.3	2.0	26.9	3.8	n.d.	5.9
CER	40.32	−5.93	0.64	49.5	n.d.	n.d.	41.1	n.d.	n.d.	9.4	n.d.	n.d.	8.6
CAR	42.49	−6.78	0.71	14.0	8.6	1.1	37.1	14.1	1.0	21.4	2.5	0.3	43.3
CAR−M	42.49	−6.79	0.73	31.0	6.2	0.4	43.1	5.8	n.d.	12.6	0.9	n.d.	5.1
SAN−C	42.13	−6.70	0.89	41.0	2.8	0.4	43.5	1.9	n.d.	10.1	0.3	n.d.	8.8
CAY	42.78	−2.99	0.94	32.6	2.9	n.d.	42.4	3.3	n.d.	18.1	0.6	n.d.	6.5
COV	43.30	−5.04	0.97	21.0	14.3	5.6	33.2	13.2	1.4	9.7	1.5	n.d.	17.8
SAN	42.13	−6.71	1.03	34.3	3.1	0.4	44.7	3.2	n.d.	13.9	0.4	n.d.	10.8
MO	42.33	1.00	1.11	25.3	7.4	1.0	40.0	8.1	n.d.	17.2	1.0	n.d.	9.2
ER	43.27	−4.98	1.13	57.3	1.8	n.d.	34.4	n.d.	n.d.	6.5	n.d.	n.d.	8.1

BGD
10, 9043–9068, 2013

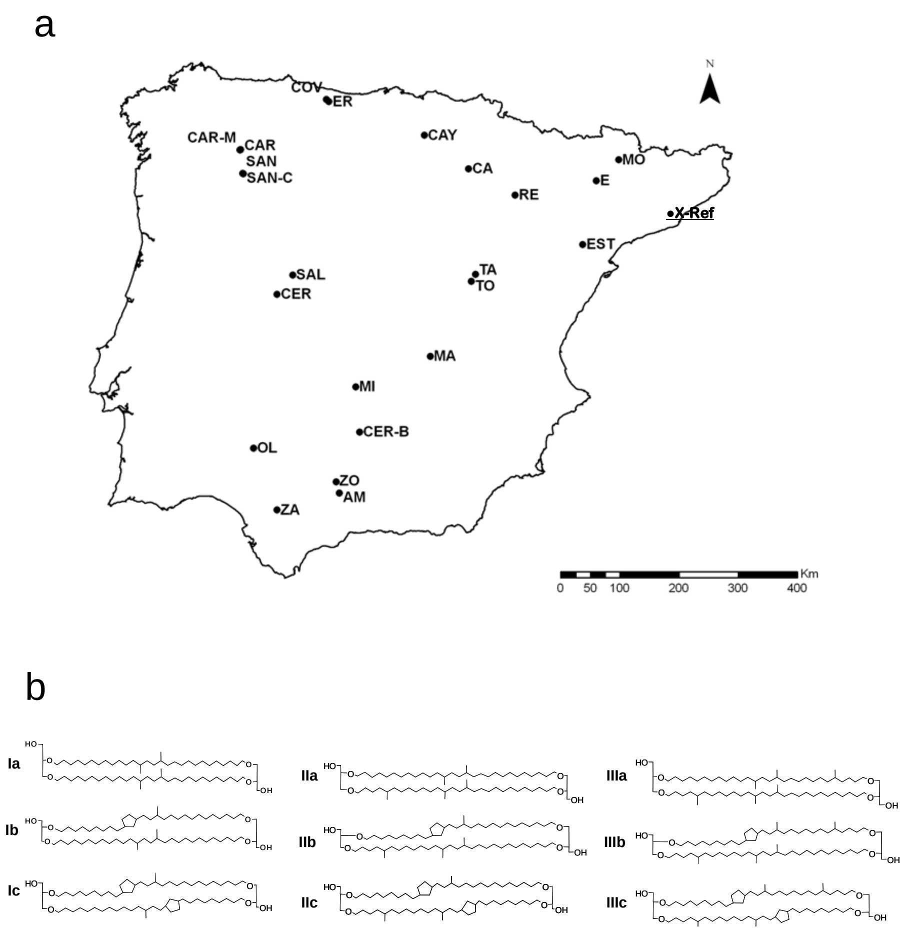

Fig. 1. (a) Map of the study area with location of surface soils and sample codes used in this study, standard soil sample X-Ref appears underlined, **(b)** brGDGT structures used in this study.

BGD
10, 9043–9068, 2013

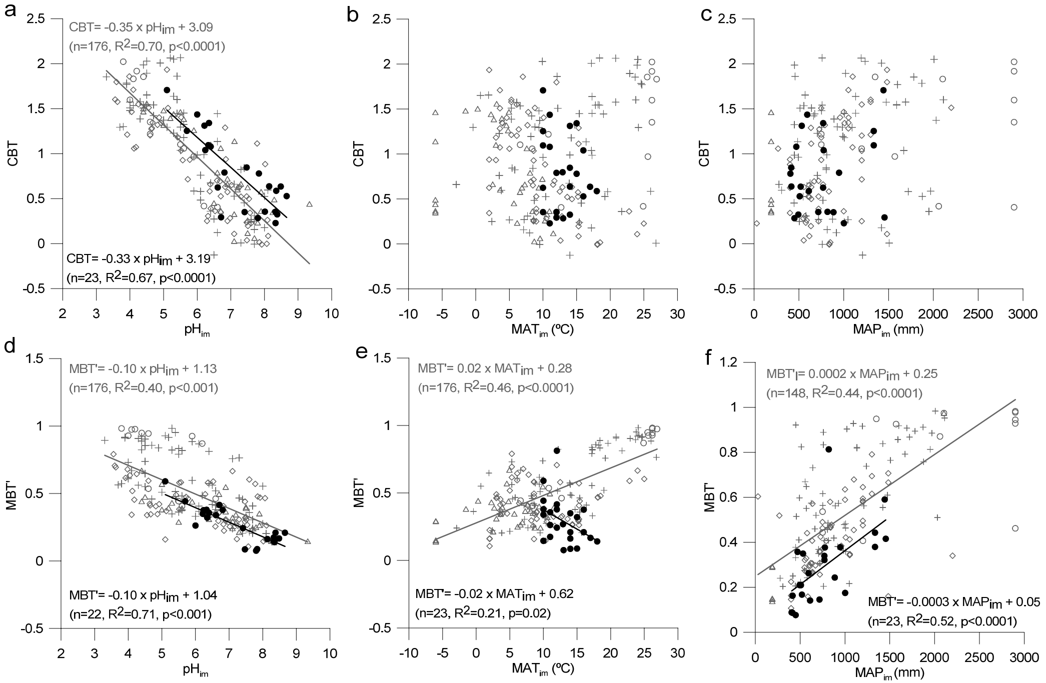

Fig. 2. Linear regression plots of **(a)** measured soil pH (pH_{im}) vs. CBT, **(b)** measured mean annual temperature (MAT_{im}; Ninyerola et al., 2005) vs. CBT, **(c)** Mean annual precipitation (MAP_{im}; (Ninyerola et al., 2005) vs. CBT, **(d)** soil pH_{im} vs. MBT', **(e)** MAT_{im} vs. MBT', and **(f)** MAP_{im} vs. MBT'. Data compiled by Peterse et al. (2012) are plotted in grey and distinguished by symbol as follows: Weijers et al. (2007) (+), Peterse et al. (2012) (◇), Bendle et al. (2010) (○) and Peterse et al. (2009b) (Δ). Data from this study are shown in black (•). Linear regression lines and equations, R^2, and p values are shown in grey for the Peterse et al. (2012) dataset, and in black for the present study.

BGD

10, 9043–9068, 2013

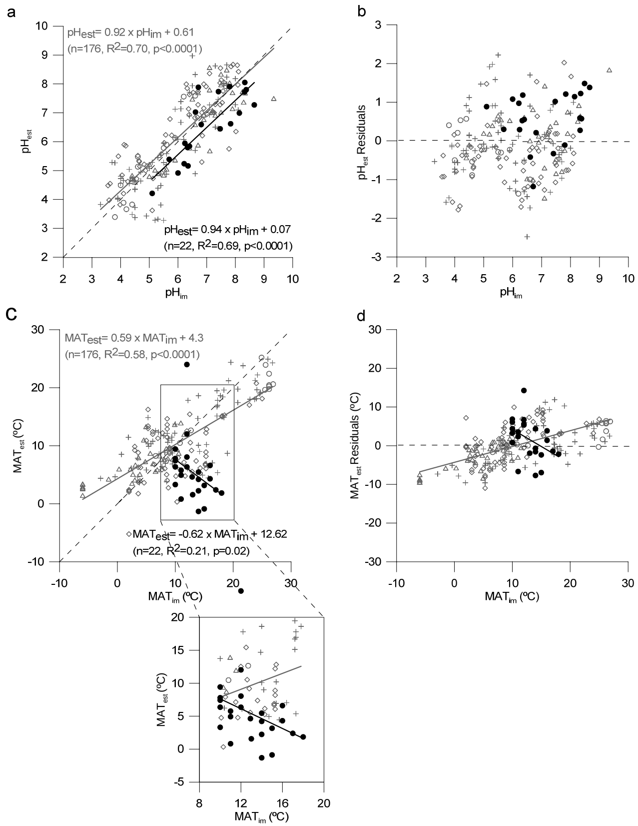

Fig. 3. Linear regression plots of **(a)** measured soil pH (pH_{im}) vs. estimated pH ($pH_{est,}$) **(b)** pH_{im} vs. pH_{est} residuals (pH_{im}-pH_{est}), **(c)** Mean Annual Temperature (MAT_{im}) vs. estimated MAT (MAT_{est}), with an insert only for the 8–20 °C MAT_{im} range, **(d)** MAT_{im} vs. MAT_{est} residuals. Data compiled by Peterse et al. (2012) are plotted in grey and distinguished by symbol as follows: Weijers et al. (2007) (+), Peterse et al. (2012) (◇), Bendle et al. (2010) (◯) and Peterse et al. (2009b) (Δ). Data from this study are shown in black (•). Linear regression lines and equations, R^2, and p values are shown in grey for the Peterse et al. (2012) dataset and in black for the present study. The dashed line is drawn for illustration purposes to indicate a 1 : 1 relationship.

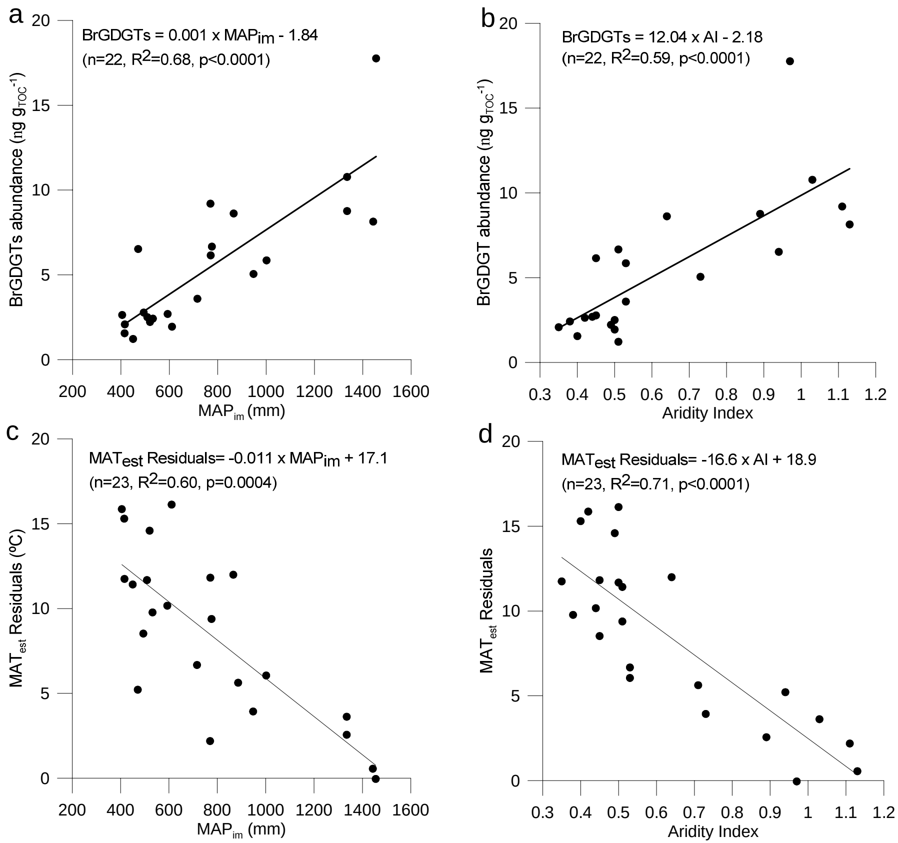

Fig. 4. Linear regression plots of **(a)** BrGDGT concentration in soils normalized to total organic carbon (TOC) vs. values of mean annual precipitation (MAP_{im}) **(b)** BrGDGT concentration normalized to TOC vs. Aridity Index (Trabucco and Zomer, 2009), **(c)** MAP_{im} vs. estimated mean annual temperature (MAT_{est}) residuals and **(d)** Aridity Index (Trabucco and Zomer, 2009) vs. MAT_{est} residuals.